International Journal of Immunopathology & Pharmacology

Original Research Article

miR-142-5p regulates the progression of diabetic retinopathy by targeting IGF1

International Journal of Immunopathology and Pharmacology
Volume 34: 1–14

DOI: 10.1177/2058738420909041
journals.sagepub.com/home/iji
SAGE

Xiuming Liu, Jianchang Li and Xiaofeng Li

Abstract

As one of leading causes of blindness, diabetic retinopathy (DR) is a progressive microvascular complication of diabetes mellitus (DM). Despite significant efforts have been devoted to investigate DR over the years, the molecular mechanisms still remained unclear. Emerging evidences demonstrated that microRNAs (miRNAs) were tightly associated with pathophysiological development of DR. Hence, this study was aimed to illustrate the role and molecular mechanisms of miR-412-5p in progression of DR. Streptozotocin (STZ) treatment in rats and human retinal endothelial cell (HREC) models were used to simulate DR conditions in vivo and in vitro. Hematoxylin-eosin (HE) staining was used to demonstrate the morphology of retinal tissues of rats. Qualitative real-time polymerase chain reaction (qRT-PCR) detected miR-142-5p and vascular endothelial growth factor (VEGF) expression levels. Cell counting kit-8 (CCK8) assay and immunofluorescence (IF) measured the cell proliferation rates. Western blot tested the expression status of IGF1/IGF1R-mediated signaling pathway. Dual-luciferase reporter assays demonstrated the molecular mechanism of miR-142-5p. miR-142-5p level was down-regulated in retinal tissues of DR rats and high glucose (HG)-treated HRECs. Insulin-like growth factor 1 (IGF1) was identified as a direct target of miR-142-5p. The reduced miR-142-5p level enhanced HRECs proliferation via activating IGF/IGF1R-mediated signaling pathway including p-PI3K, p-ERK, p-AKT, and VEGF activation, ultimately giving rise to cell proliferation. Either miR-142-5p overexpression or IGF1 knockdown alleviated the pathological effects on retinal tissues in DR rats. Collectively, miR-142-5p participated in DR development by targeting IGF1/p-IGF1R signaling pathway and VEGF generation. This miR-142-5p/IGF1/VEGF axis provided a novel therapeutic target for DR clinical treatment.

Keywords

diabetic retinopathy, IGF1, miR-142-5p, VEGF

Date received: 22 April 2019; accepted: 21 January 2020

Introduction

As one of the leading complications of diabetes mellitus (DM), diabetic retinopathy (DR) is characterized by progressive microvascular deficit in the retina caused by chronic hyperglycemia.[1,2] DR is considered a disease with high incidences throughout the world, especially in developed countries,[3] as it exhibited no obvious clinical symptoms in early stage, and it could not be precisely diagnosed until the advanced stage.[4] Despite progresses archived in DR therapy in past two decades, prognosis of DR still remains largely unclear.[5] Hence, it is urgent to investigate the potential molecular mechanisms underlying DM progression for clinical therapy.

Recently, it is reported that altered microRNA (miRNA) levels are tightly associated with signaling pathways during the DR progression.[6,7] miRNAs are a family of short noncoding RNAs with ~22

Department of Ophthalmology, The Affiliated Huaian No.1 People's Hospital of Nanjing Medical University, Huai'an, China

Corresponding author:
Xiuming Liu, Department of Ophthalmology, The Affiliated Huaian No.1 People's Hospital of Nanjing Medical University, Huai'an 223300, Jiangsu, China.
Email: LiuxiumingLLL@163.com

nucleotides long and highly conserved sequences that inhibited protein translation by targeting its 3′ untranslated region (UTR) or promoted its mRNA degradation.[8] miR-142 is considered as a crucial miRNA in regulating a variety of cell biology activities. It functions as a major modulator in the hematopoietic system and embryonic development.[9–11] Moreover, miR-142 participates in regulation of various diseases including cancer, inflammation, immune tolerance, and virus infection.[9,12] miR-142-5p was found to be inhibited in retinal tissues of streptozotocin (STZ)-treated rats according to miRNA microarray analysis.[13] However, the precise functions and molecular mechanisms of miR-142-5p in DR remained unknown.

Insulin-like growth factor 1 (IGF1) is a critical growth and transcriptional factor that is linked with cell proliferation/survival and the development of angiogenesis.[14,15] IGF1/IGF1-binding proteins (IGF1BPs) and vascular endothelial growth factor (VEGF) contribute to regulation of diabetic angiopathy in DM animal models and patients.[16,17] In high-glucose (HG) treated human retinal endothelial cell (HREC) models, IGF1/IGF1R was derepressed by the reduced miR-18b level, subsequently activated VEGF secretion and that consequently initiated the downstream phosphorylation of Akt, MEK, and ERK.[18] Powerful experimental and clinical findings suggested IGF1 was tightly related to DR development. However, additional data are required to validate the potential regulatory mechanisms of IGF1 in the pathogenesis of DR. In this study, we elucidated the functions of miR-142-5p/IGF1/VEGF signaling axis in the pathogenic processes of DR in vivo and in vitro.

Method and materials

DR animal model establishment

Male Sprague–Dawley (SD) rats (~8 weeks) were purchased from Shanghai SLAC Laboratories Inc (Shanghai, China). Those rats were kept in a pathogen-free environment under 12 h:12 h day/light cycle at a temperature of 25°C. All rats had free access to adequate food and purified water. All experimental procedures were performed according to the Guide for the Care and Use of Laboratory Animals and were approved by the Animal Care and Use Committee of the Affiliated Huaian NO.1 People's Hospital of Nanjing Medical University.

The rats were randomly assigned to DR and sham group (DR, n = 36, Sham, n = 8). The DR group received a 60 mg/kg intraperitoneal injection of STZ dissolved in 0.1 mol/L citrate buffer. The sham group was intraperitoneally administered with the same volume of citrate buffer (0.1 mol/L). After STZ injection for 72 h, rats exhibited high blood glucose concentration (>16.7 mM) after fasting overnight were regarded as successfully established diabetic models in our study.

The rats in DR group (n = 28) were randomly distributed into four groups for the treatment study: ① DR + miR-NC (n = 7), ② DR + miR-142-5p (n = 7), ③ DR + si-NC (n = 7), and ④ DR + siIGF1 (n = 7). miR-142-5p or miR-NC (2 μg/eye/week), as well as siIGF1 or si-NC were administrated into the eye of the DR rats using inviofectamine 3.0 Reagent (Invitrogen, Carlsbad, USA) according manufacture's protocols. About 10 weeks post injection, all rats were sacrificed to collect the retinal tissues for the further study.

Cell culture

HRECs were purchased from Olaf (Worcester, MA, USA). Cells were cultured in human microvascular endothelial medium (Cell applications, Inc, San Diego, USA) at 37°C in a humidified atmosphere supplemented with 5% CO_2. Experiments were carried out among cell passages 3 and 8. Cells seeded in six-well plates were treated with high concentration of glucose (25 mM D-glucose) or normal concentration of glucose (NG, 5 mM D-glucose) for 3 days.

Human embryonic kidney 293 (HEK293) cells were acquired from American Type Culture Collection (ATCC, Manassas, USA). Cells were cultured in Dulbecco's modified Eagle's medium (DMEM, Gibco, Carlsbad, USA) with 10% fetal bovine serum (FBS, Gibco) and 100 U/mL penicillin/streptomycin (Gibco) in 5% CO_2 humidified atmosphere at 37°C.

Transfection and drug treatment

HRECs were transfected with miR-142-5p (GenePharma, Shanghai, China) or miRNA-negative control (miR-NC), miR-142-5p-inhibitor (miR-142-5p-inh), or miR-NC-inhibitor (miR-inh), siIGF1, or si-NC, as well as IGF1 overexpression pcDNA3.1 plasmid using the Lipofectamine

Table 1. The primers for qRT-PCR and siRNA were listed in the study.

Name	Primer	Sequence (5′-3′)
VEGF	Forward	5′-GAAGTGGTGAAGTTCATGGA-3′
	Reverse	5′-GCCTTGCAACGCGAGTCTGT-3′
β-Actin	Sense	5′-CCAGCACCATGAAGATCAAGATC-3′
	Anti-sense	5′-ACATCTGCTGCTGGAAGGTGGACA-3′
miR-142-5p	Forward	5′-AACTCCAGCTGGTCCTTAG-3′
	Reverse	5′-TCTTGAACCCTCATCCTGT-3′
U6	Forward	5′-CTCGCTTCGGCAGCACA-3′
	Reverse	5′-AACGCTTCACGAATTTGCGT-3′
siIGF1	Target	5′-GTCCTCCTCGCATCTCTTCTA-3′
	Anti-sense	5′-GCCCTCATCGCTATTCTCTCT-3′

VEGF: vascular endothelial growth factor.

2000 Reagent (Invitrogen) following the manufacturer's instructions. About 24 h post transfection, cells were treated with HG (25 mM) for 48 h, and then HRECs were collected for further study. In addition, cells were treated with the inhibitors of MEK (PD0325901, 200 nM, Selleck chemicals, Houston, USA) and PI3K (LY294002, 20 μM, Beyotime Biotechnology, Shanghai, China), as well as activator of AKT (SC79, 4 μg/mL, Selleck chemicals), respectively for molecular mechanism testing experiment.

HE staining

After fixation in polyformaldehyde (4%), dehydration by conventional gradient, permeation by xylene, and embedding in paraffin, the eye tissues were cut into sections with 5 μm. The retinal morphological characteristics were determined by hematoxylin-eosin (HE, Solarbio, Beijing, China) staining. The morphologic images of retinal membrane tissues were obtained using Olympus microscope (Tokyo, Japan).

Immunofluorescence staining

After fixation overnight, eyes were cut into 15 μm coronal sections using a freezing microtome (Leica, Solms, Germany). First, the sections were incubated in blocking buffer containing 10% normal goat serum and 0.2% Triton X-100 dissolved in phosphate-buffered serum (PBS) for 1 h at room temperature. With the primary antibodies, the sections were probed by anti-CD31 antibody (1:50 dilution, Abcam, Cambridge, UK), anti-vWF antibody (1:300 dilution, Abcam), anti-VE-cadherin antibody (1:500 dilution, Abcam) or anti-Ki-67 antibody (1:100 dilution, Abcam) overnight at 4°C following by incubation with Alexa Fluor 488–conjugated goat anti-rabbit antibody (1:500 dilution, Jackson ImmunoResearch laboratories, Inc, West Grove, USA) or Cy3-conjugated goat anti-rabbit antibody (1:500, Jackson ImmunoResearch laboratories, Inc) for 1 h at room temperature. Then the sections were mounted on glass slides and visualized with Leica fluorescence microscope (DMI3000, Leica). A slide without primary antibody was regarded as the negative control. Exposure conditions in the same channel of different groups in each experiment were kept the same.

Quantitative real-time PCR

Total RNAs were extracted from tissues or cells using TRIzol reagent (Invitrogen) following the reagent instructions and quantified using a NanoDrop 2000 (Thermo Fisher, Waltham, USA). Complementary DNA (cDNA) was synthesized using an RNA plate using miRNA cDNA Synthesis Kit (TaKaRa, Dalian, China). Real-time polymerase chain reaction (PCR) was executed using Script SYBR Green PCR Kit (TaKaRa). β-Actin or U6 small nuclear RNA were served as internal controls for quantification of VEGF or miR-142-5p, respectively. Relative levels of mRNA or miRNA were evaluated using $2^{-\Delta\Delta ct}$ method. Primers used in this study were synthesized by Shanghai Sangon Biotech (Shanghai, China) and listed in Table 1. Experiments were repeated at least three times.

Western blotting

Proteins were lysed with RIPA buffer (Beyotime Biotechnology) for 30 min on the ice and then centrifuged at 10,000 r/min for 20 min at 4°C. Then protein concentration was determined using a

Bicinchoninic acid (BCA) kit (Beyotime Biotechnology). A small amount of (30 μg) protein was separated by sodium dodecyl sulfate–polyacrylamide gel electrophoresis (SDS-PAGE) and transferred onto polyvinylidene fluoride (PVDF) membrane (Bio-Rad, Hercules, USA). Next, the membrane was incubated with blocking buffer, and incubated overnight at 4°C with the corresponding primary antibodies: anti-IGF1 antibody (1:500 dilution, Abcam), anti-p-IGF1R antibody (1:500 dilution, Abcam), anti-IGF1R antibody (1:1000 dilution, Abcam), p-MEK antibody (1:2000 dilution, Abcam), anti-MEK antibody (1:2000 dilution, Abcam), anti-p-AKT antibody (1:5000 dilution, Abcam), anti-AKT antibody (1:10000 dilution, Abcam), anti-p-ERK1/2 antibody (1:300 dilution, Abcam), anti-ERK1/2 antibody (1:1000 dilution, Abcam), anti-VEGF antibody (1:500 dilution, Abcam), anti-Tubulin antibody (1:5000 dilution, Abcam), then probed with horseradish peroxidase–labeled secondary antibodies (1: 1000 dilution, Beyotime Biotechnology) for 1 h at room temperature. The protein bands were visualized by enhanced chemiluminescence (Millpore), and the optical intensity were determined by Quantity One software (Bio-Rad). Experiments were repeated at least three times

Cell counting kit-8 assay

Cell counting kit-8 (CCK8) assay was performed to evaluate the cell viability or proliferation. HRECs ($1*10^4$) were seeded and cultured in 96-well plates overnight. An aliquot of CCK8 (10 μL, Dojindo, Kumamoto, Japan) was subsequently added into each well and incubated for 2 h at 37°C. To quantify the numbers of viable cells in each well, the absorbance was detected at a wavelength of 450 nm using Synergy 2 multimode microplate reader (BioTek, Vermont, USA). All the experiments were repeated three times in triplicate.

Dual-luciferase assay

The fragment of IGF1 mRNA 3′UTR containing the predicted miR-142-5p binding site (IGF 3'UTR-WT) or the corresponding mutant produced by mutating the miR-142-5p seed region binding site (IGF 3′UTR-MUT were obtained by The Beijing Genomics Institute BGI (Beijing, China). Then fragments were inserted into a pmirGLO Dual-luciferase Vector (Promega, Madison, USA). The miR-142-5p mimic or miR-NC were co-transfected with the luciferase reporter vectors, respectively into the HEK293 cells following adding pRL-TK vector using Lipofectamine 2000 (Invitrogen). The relative luciferase activity was estimated using the Dual-Luciferase Reporter Assay System (Promega) 48 h post transfection. Experiments were repeated at least three times

Statistical analysis

Statistical analysis was performed using SPSS 21.0 (SPSS, Inc, Chicago, IL). The comparisons between two groups were evaluated by a two-tailed Student's t-test and multiple groups differences were determined by one-way analysis of variance (ANOVA) followed by Bonferroni's multiple comparison tests. All data are expressed as the mean ± standard deviation (SD). P values <0.05 were considered as statistically significant in this study ($*P<0.05$, $**P<0.01$, $***P<0.001$).

Results

miR-142-5p level was decreased in retinal tissues of DR rats or in HG-induced HRECs

First, the pathologic alterations of retinal tissues were compared between DR group and normal group using HE staining. As shown in Figure 1(a), the structure and cell layers of retinal tissue were integrated and clear in the normal group (n=2). The cell number was abundant, and the cell morphology was intact and arranged neatly. However, in the DR group, the inner and outer nuclear layers of the retina were blurred, and the nerve fiber layer was edema. Moreover, the number of retinal cells was reduced and the cells arranged sparsely and disorderly. The morphology of HRECs were identified as goose-oval using phase contrast microscope (Figure 1(b)), and the vascular endothelium markers-CD31, von Willebrand factor (vWF) and VE-cadherin were positively expressed in cell lines of HRECs (Figure 1(c)). Next, miR-142-5p expression was detected using qualitative real-time polymerase chain reaction (qRT-PCR) under DR pathological condition in vivo and in vitro. miR-142-5p level was significantly down-regulated in retinal tissues of DR rats compared to that of normal rats ($***P<0.001$, n=6, Figure 1(d)). In addition, the expression of miR-142-5p was remarkably decreased in HRECs in HG-treated group compared with NG group

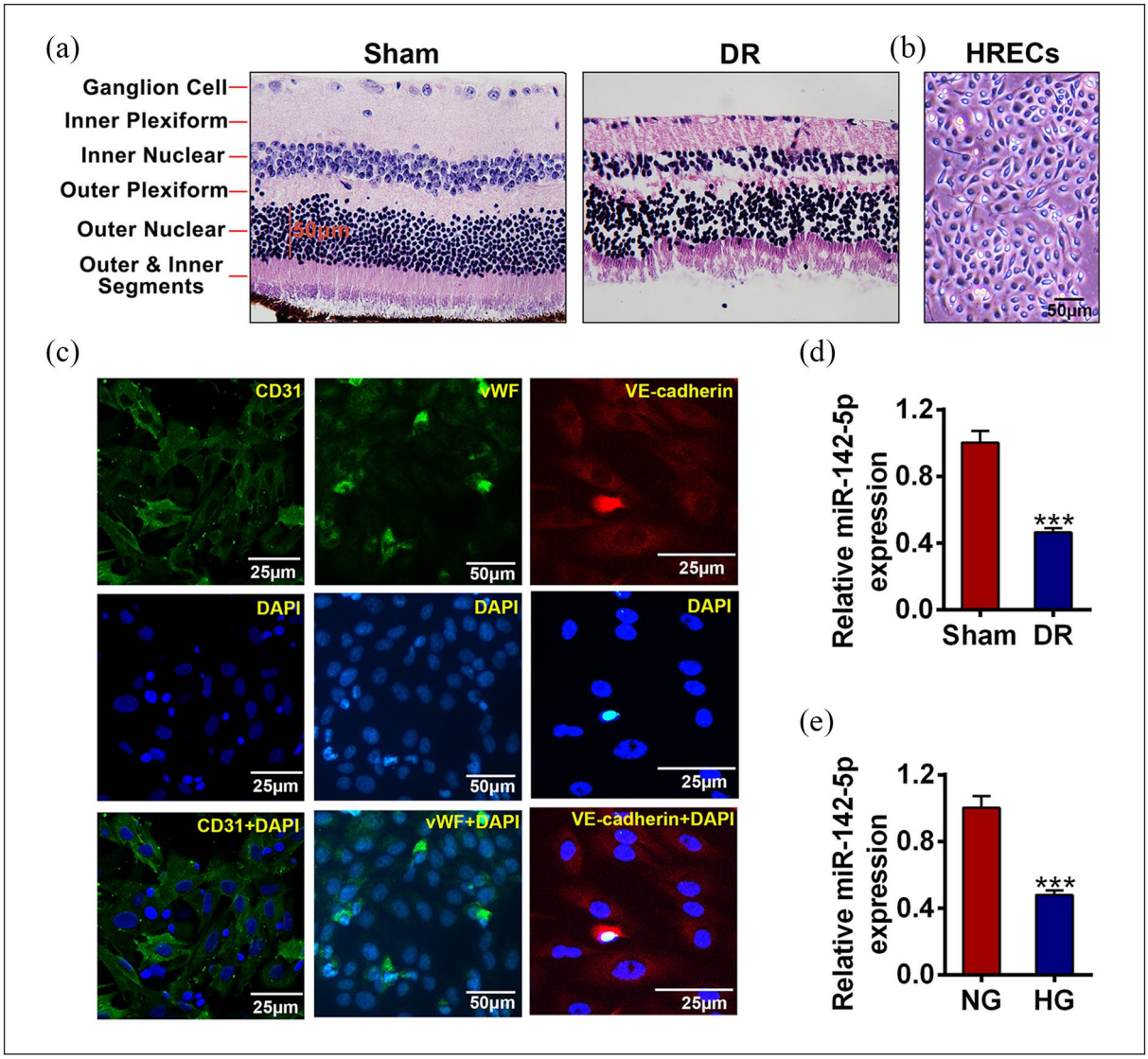

Figure 1. miR-142-5p level was decreased in retinal tissues of DR-treated rats and in HG-treated HRECs. (a) Representative photos showing the pathological characteristics of retinal tissues in sham and DR group using HE staining. Scale bar = 50 μm. n = 2. (b) Representative image showing the HRECs. Scale bar = 50 μm. (c) Expression levels of markers including CD31, vWF, and VE-cadherin in HRECs was detected by IF method. Scale bar = 25 μm (CD31, VE-cadherin staining). Scale bar = 50 μm (vWF staining). (d) miR-142-5p levels in retinal tissues in sham and DR group of rats were determined by qRT-PCR (n = 6). (e) The miR-142-5p levels of HRECs in NG and HG group were tested by qRT-PCR (mean ± SD; ***$P < 0.001$).

(***$P < 0.001$, Figure 1(e)). Taken together, the DR rat model was successfully established and the characteristics of HRECs were well identified, and miR-142-5p level was down-regulated under DR pathological condition.

miR-142-5p suppressed HG treatment–induced HRECs proliferation

Next, the effects of miR-142-5p on the retinal cell growth were examined in cell lines of HRECs. First, we confirmed that the decreased miR-142-5p level was restored by its mimics under HG treatment compared with miR-NC group (***$P < 0.001$, Figure 2(a)). To determine whether VEGF was associated with the change expression of miR-142-5p, qRT-PCR assays were performed. As shown in Figure 2(b), VEGF level was enhanced upon HG treatment, while decreased by miR-142-5p mimic compared with miR-NC group (*$P < 0.05$). Furthermore, the effect of altered miR-142-5p expression level on the cell proliferation was measured by CCK8 and immunofluorescence (IF) assay. The cell viability was decreased

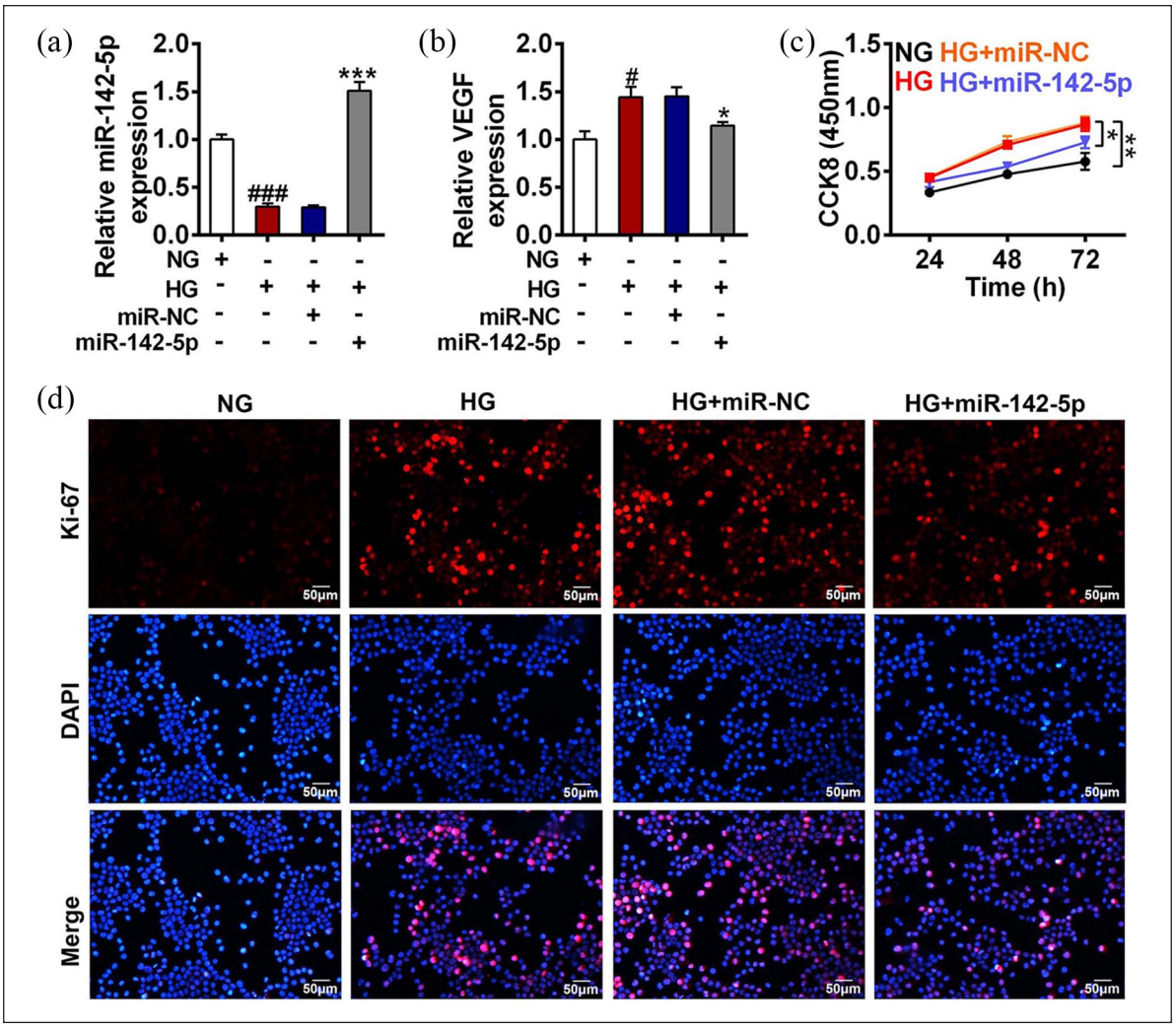

Figure 2. miR-142-5p inhibited HREC proliferation induced by HG treatment. Cell lines of HRECs were transfected with miR-142-5p or miR-NC for 24 h followed by HG exposure. (a and b) The influence of miR-142-5p mimics on miR-142-5p and VEGF levels were measured by qRT-PCR upon HG treatment. (c) Effects of miR-142-5p overexpression on the HRECs viability were evaluated by CCK8 under HG conditions. (d) Effects of miR-142-5p mimic on the Ki-67 staining was assessed by IF assay insult to HG treatment. Scale bar = 50 μm. (mean ± SD; $^{*}P < 0.05$, $^{**}P < 0.01$, $^{***}P < 0.001$, $^{\#}P < 0.05$, $^{\#\#\#}P < 0.001$).

under miR-142-5p overexpression compared with miR-NC treatment upon HG treatment ($^{**}P < 0.01$, $^{*}P < 0.05$, Figure 2(c)). Conformably, the expression of cell proliferation marker-Ki-67 was enhanced under HG treatment, while such enhancement could be inhibited by miR-142-5p mimic in HG-treated cells (Figure 2(d)). Altogether, up-regulated miR-142-5p expression prevented cell proliferation upon HG treatment in HRECs.

IGF1 was a direct target of miR-142-5p

miRNAs normally execute their functions through targeting the 3′UTR of mRNAs to modulate downstream protein levels.[8] An online analysis software named Targetscan (http://www.targetscan.org/) predicted a binding site between the 3′UTR of IGF1 mRNA and the miR-142-5p seed sequence (Figure 3(a)). To validate whether IGF1 is a target of miR-142-5p, the fragment of IGF1 mRNA 3′UTR–containing WT or MUT miR-142-5p-binding site was cloned to the luciferase reporter plasmid, respectively, which accompanying with miR-142-5p or miR-NC were co-transfected with the HEK293 cells (Figure 3(b)). The luciferase activity of HEK293 cells treated with IGF 3′UTR WT vector was significantly attenuated by miR-142-5p, while there was no remarkably difference between cells co-treated with IGF 3′UTR MUT vector and miR-142-5p (IGF1 3′UTR-WT: $^{***}P < 0.001$, IGF1 3′UTR-MUT:

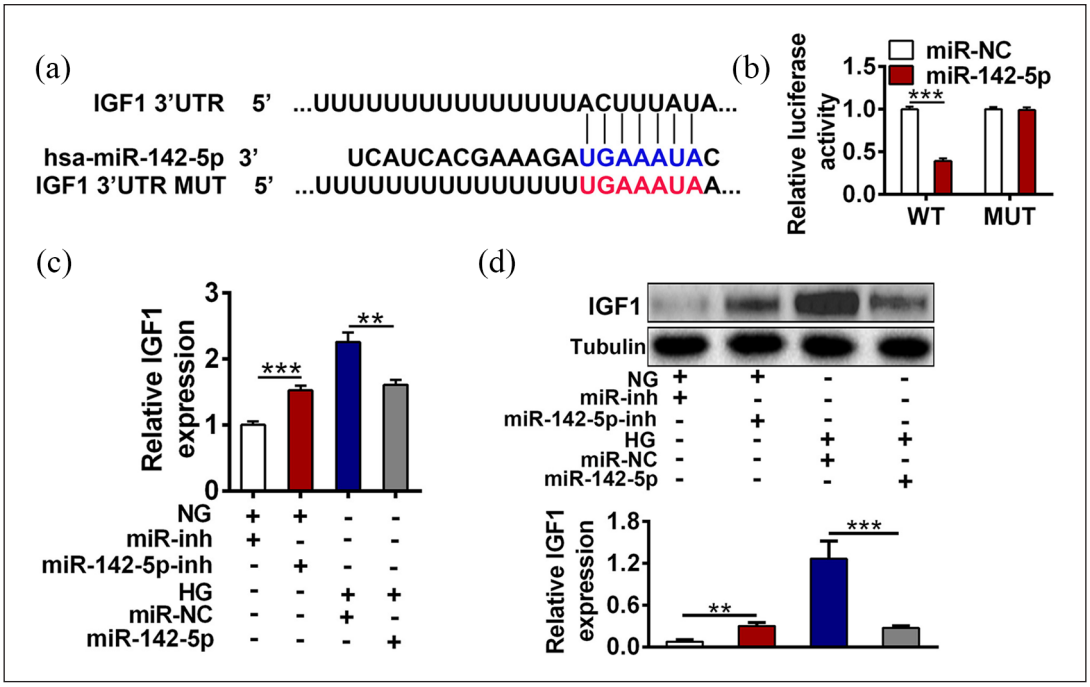

Figure 3. miR-142-5p directly targeted IGF1. (a) The seed sequence of miR-142-5p targets the WT or MUT 3′UTR of IGF1 mRNA. (b) Luciferase activity of HEK293 cells co-transfected with miR-142-5p or miR-NC and luciferase reporters of IGF1 mRNA 3′UTR-WT or -MUT vector were checked by dual-luciferase reporter assays. (c and d) The influence of inhibition of miR-142-5p level upon NG condition and up-regulation of miR-142-5p level under HG treatment on the expressions of IGF1 mRNA or protein levels were measured by qRT-PCR or Western blot methods, respectively (mean ± SD; $^{**}P<0.01$, $^{***}P<0.001$).

$P>0.05$, Figure 3(b)). Furthermore, the influence of change miR-142-5p expression on the IGF1 translation level was examined using qRT-PCR and Western blot. The mRNA and protein levels of IGF1 were strengthened by miR-142-5p inhibitor compared with miR-inhibitor group ($^{***}P<0.001$, $^{**}P<0.01$, Figure 3(c) and (d)) and decreased by miR-142-5p mimic compared with miR-NC group under HG treatment ($^{***}P<0.001$, $^{**}P<0.01$, Figure 3(c) and (d)). These data suggested that IGF1 was directly targeted by miR-142-5p.

miR-142-5p modulated VEGF expression by targeting the IGF1/IGF1R-mediated signaling upon HG treatment

To explore whether the downstream factors of IGF1 participate in regulating the progression of DR, we investigated the role of miR-142-5p and IGF1 in IGF1/IGF1R-mediated signaling as well as subsequently VEGF level using Western blot. As shown in Figure 4(a), the protein levels of p-IGF1R/IGF1R, p-MEK/MEK, p-AKT/AKT, p-ERK1/2/ERK1/2, and VEGF were enhanced by miR-142-5p inhibitor but further inhibited by interference of IGF1 level in NG HRECs ($^{***}P<0.001$, $^{*}P<0.05$). In addition, the protein levels of p-IGF1R/IGF1R, p-MEK/MEK, p-AKT/AKT, p-ERK1/2/ERK1/2, and VEGF were decreased by miR-142-5p mimic compared with miR-NC group under HG treatment, while further up-regulated by IGF1 overexpression ($^{***}P<0.001$, $^{**}P<0.01$, $^{*}P<0.05$, Figure 4(b)). Altogether, the reduced miR-142-5p level would enhance the VEGF expression via activating the IGF1/IGF1R-mediated signaling pathway under HG treatment.

miR-142-5p regulated cell proliferation via targeting the IGF1/IGF1R-mediated signaling under HG-treated condition

To investigate whether miR-142-5p modulated cell viability through IGF1/IGF1R-mediated signaling pathway, Western blot and CCK8 and Ki-67 staining were performed in HRECs, co-transfected with miR-142-5p mimics or inhibitor and the antagonists of MEK, PI3K, or the agonist of AKT. As shown in Figure 5(a) and (b), the elevated levels of VEGF induced by miR-142-5p inhibitor were re-inhibited

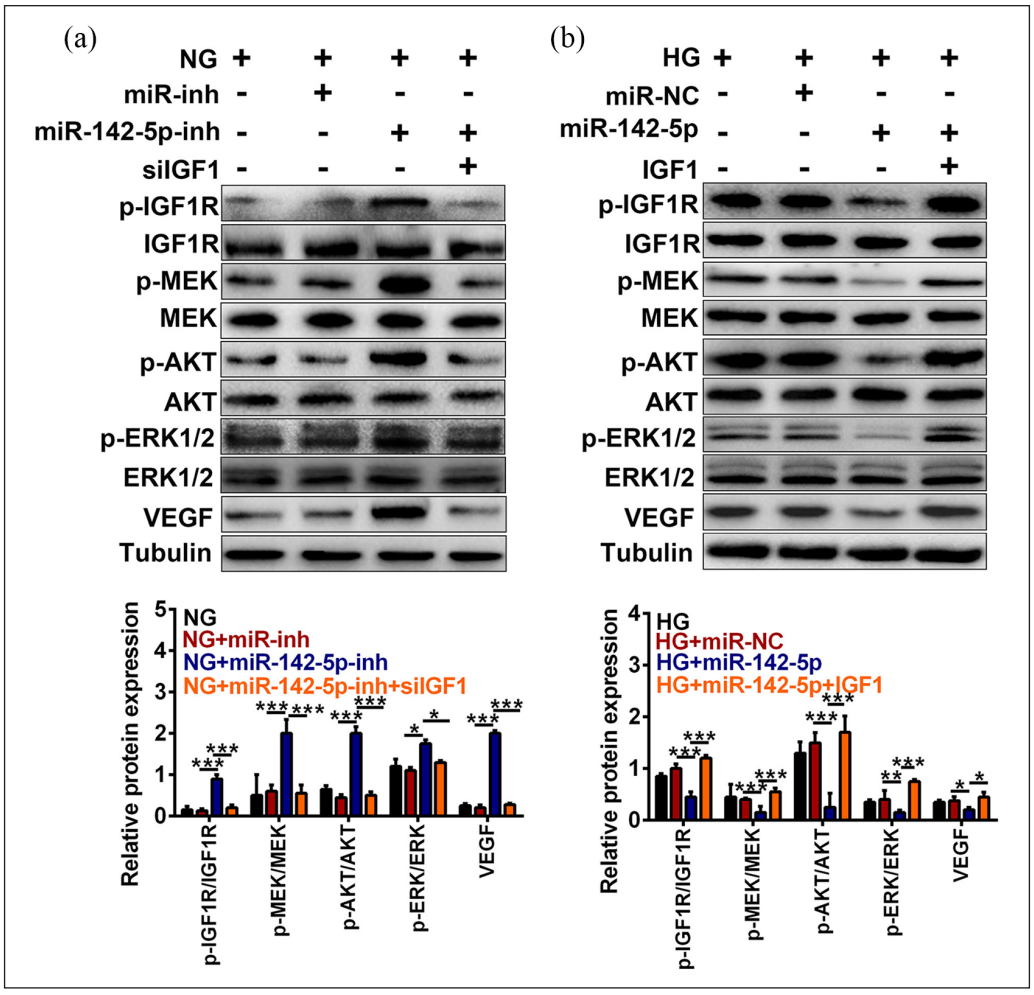

Figure 4. Decreased miR-142-5p expression enhanced VEGF level via activating the IGF1/IGF1R-mediated signaling under HG treatment. (a) Influences of miR-142-5p inhibitor with/without IGF1 knockdown on the expressions of p-IGF1R/IGF1R, p-MEK/MEK, p-AKT/AKT, p-ERK1/2/ERK1/2, and VEGF were examined by Western blot. (b) Effect of miR-142-5p mimic with/without IGF1 overexpression on the expressions of p-IGF1R/IGF1R, p-MEK/MEK, p-AKT/AKT, p-ERK1/2/ERK1/2, and VEGF were quantified by Western blot. (mean ± SD; $*P < 0.05$, $**P < 0.01$, $***P < 0.001$).

by PI3K inhibitor-LY294002 or MEK inhibitor PD032501, respectively, in NG-treated HRECs ($***P < 0.001$, $*P < 0.05$). In addition, the weakened expression of VEGF induced by miR-142-5p mimic under NG treatment could be rescued by AKT activator SC-79 in HRECs cells ($***P < 0.001$, Figure 5(c)). Furthermore, the heightened cell viability proved by CCK8 assay induced by miR-142-5p inhibitor were further abated by PI3K or MEK inhibitor in NG-treated cell, respectively ($**P < 0.01$, Figure 5(d)), while cell viability decreased by miR-142-5p mimics was promoted by SC-79 ($**P < 0.01$, Figure 5(e)). Consistently, the Ki-67-positive cells were elevated by down-regulation of miR-142-5p expression, whereas further attenuated by PI3K inhibitor-LY294002 or MEK inhibitor-PD032501 in NG cells (Figure 5(f) and (g)). The lessened cell proliferation proved by Ki-67 staining assays induced by overexpression of miR-142-5p were further enhanced by AKT agonist SC-79 in HG-treated HRECs ($**P < 0.01$, Figure 5(h)). In summary, altered miR-142-5p level mediated cell proliferation by regulating PI3K/AKT/MEK pathway.

Elevated miR-142-5p level exerts protective functions in retinal tissue of DR-treated rats via targeting IGF1

The activation of IGF1/IGF1R-mediated signaling in retinal tissue of DR-treated rats was suppressed upon miR-142-5p mimic treatment or IGF1 knockdown ($***P < 0.001$, $**P < 0.01$, $*P < 0.05$, n = 7, Figure 6(a)). Furthermore, the pathological morphology of retinal tissues of DR

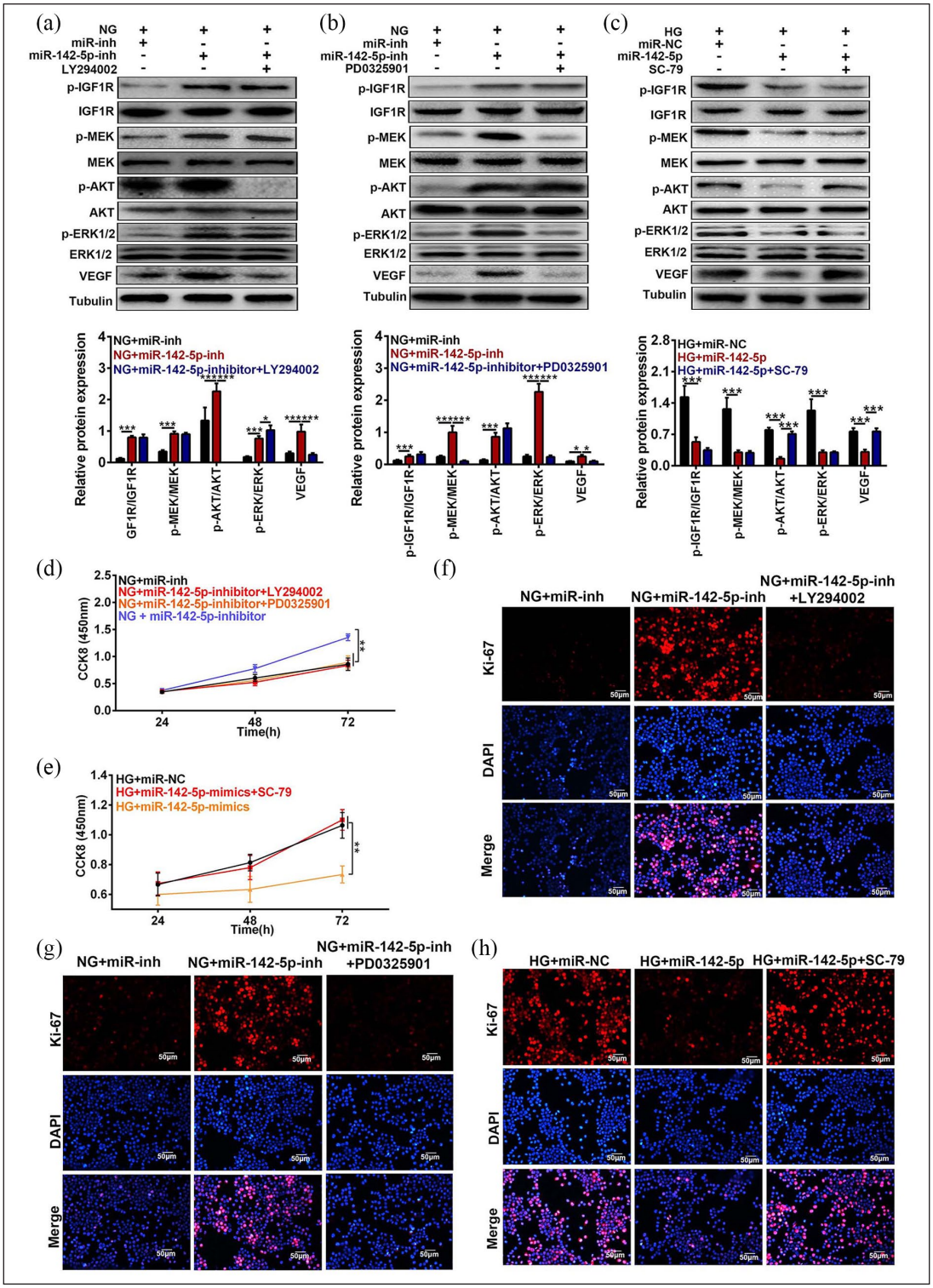

Figure 5. Effects of changed miR-142-5p expression along with MEK, AKT, and PI3K inhibitors on HREC proliferation. (a and b) Influences of suppressed miR-142-5p level with PI3K inhibitor LY294002 or MEK inhibitor PD0325901 on the IGF1/IGF1R-mediated signaling pathway and VEGF levels were detected by Western blot method under NG condition. (c) Role of enhanced miR-142-5p level accompanying with AKT agonist SC-79 in the expressions of IGF1/IGF1R-mediated signaling pathway and VEGF levels were measured by Western blot assay to HG treatment. (d) Effects of prohibition the miR-142-5p level meanwhile with treatment of LY294002 or PD0325901 on the HRECs viability were tested by CCK8 assay under NG treatment. (e) Influences of miR-142-5p mimic following with SC-79 treatment on the HRECs proliferation were examined by CCK8 assay upon HG treatment. (f and g) Functions of co-treatment of miR-142-5p inhibitor and PI3K, MEK inhibitor on Ki-67 levels were checked by IF assay, respectively. (h) Effects of co-treated miR-142-5p mimic and AKT activator were measured by IF method under HG condition. Scale bar = 50 μm. (mean ± SD; $^{*}P < 0.05$, $^{**}P < 0.01$, $^{***}P < 0.001$).

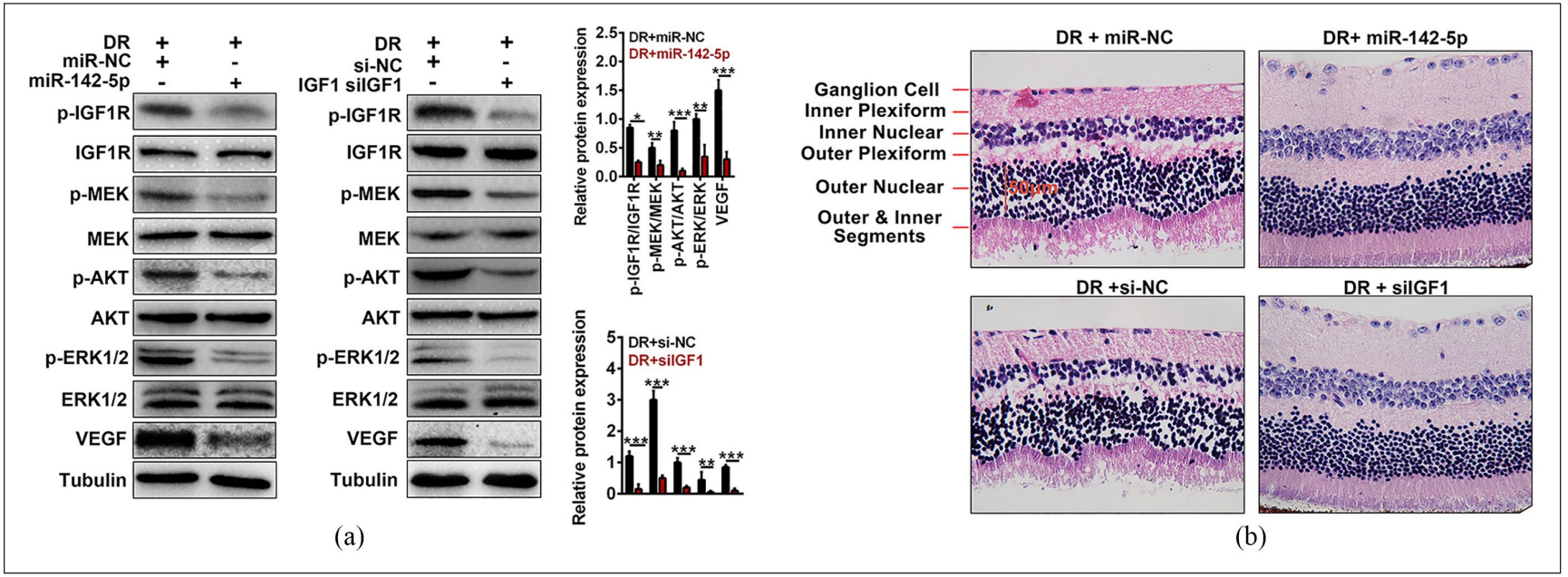

Figure 6. miR-142-5p improved the retinal functions via targeting IGF1 expression in DR-treated rats: (a) Effects of miR-142-5p mimic or siIGF1 on the IGF1/IGF1R-mediated signaling pathway and VEGF levels were detected by Western blot in the retinal tissue of DR-treated rats (n = 7). (b) Influences of miR-142-5p overexpression or IGF1 knockdown on the morphology of retina in DR-treated rats were measured by HE staining. Scale bar = 50 μm (mean ± SD; $^{*}P < 0.05$, $^{**}P < 0.01$, $^{***}P < 0.001$).

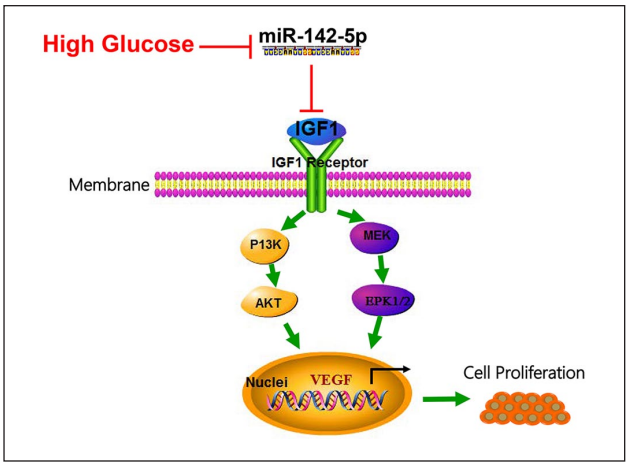

Figure 7. Schematic representation of the function of miR-142-5p and IGF1/IGF1R-mediated signaling pathway axis in the progression of DR.
HG-induced DR pathological state suppressed miR-142-5p expression which targets IGF1/IGF1R. IGF1 disinhibited when miR-142-5p restrained under HG condition and thus activating PI3K/AKT and MEK/ERK1/2 signaling pathway, therefore initiating VEGF transcription and cell proliferation.

rats would be alleviated by miR-142-5p overexpression or IGF1 knockdown (Figure 6(b)). Altogether, restored miR-142-5p level could protect cells from damage of retinal tissue of DR rats caused by IGF1.

Discussion

DR exhibits multiple negative impacts on patient's life, which has been considered as a major cause of blindness in Western developed countries.[19] To date, miRNAs and their potential regulatory networks have been reported to function as critical modulators in the pathogenesis of DM and related complications.[20] This study demonstrated that miR-142-5p was down-regulated in retinal tissues of DR rats and HG-treated HRECs. IGF1 is a direct target of miR-142-5p. The attenuated miR-142-5p level activated IGF/IGF1R-mediated signaling pathway including p-PI3K, p-ERK, p-AKT, and VEGF generation, ultimately giving rise to cell proliferation (Figure 7). miR-142-5p overexpression or IGF1 knockdown could alleviate the pathological impairments of retinal tissue in DR-treated rats.

miRNAs exert multiple types of functions including regulation of inflammatory, oxidative stress, angiogenesis, and coagulation in the progression and development of DR.[21–23] For instance, the ectopic expressions of miR-21-5p, miR-365, miR-495, or miR-211 promoted cell proliferation and angiogenesis in DR by modulation of maspin/AKT/ERK, Timp3, Notch/PTEN/Akt, or Sirtuin 1, respectively,[24–27] while miR-384-3p, miR-145, miR-133b, or miR-181a suppressed retinal neovascularization, oxidative stress, inflammation, and cell proliferation via restraining hexokinase 2, TLR4/NF-κB, ras homolog family member A, or VEGF expressions, respectively.[28–30] Although miR-142 has been considered as one of leading functional miRNAs in various cellular events, studies reported that miR-142-5p was implicated in occurrence and progression of DM and its complications.[9,12] In DM human subjects as well as in mouse models, miR-142 level was reduced.[31] Moreover, miR-142-5p level was elevated in type 2 diabetics upon TianMai Xiaoke tablet (TM) treatment.[32] In addition, miRNA microarray analysis suggests that miR-142-5p expression was down-regulated in retinal tissues of STZ-treated rats.[13] Consistently, our present data reported that miR-142-5p level was inhibited in retinal tissue of DR-treated rats as well as in HG-treated HRECs. The decreased miR-142-5p level resulted in the promotion of HREC proliferation, and miR-142-5p overexpression alleviated retinal damages caused by DR treatment. On the basis of our findings, we propose that miR-142-5p functions as a protector during progression of DR. However, there should be a preliminary miRNA chip data to screen the dysregulated miRNAs in DR pathological condition not only miR-142-5p. Moreover, a lack of clinical data in the paper, as it is better to detect the expression of miR-142-5p in clinical samples, otherwise it could be developed as a novel therapeutic candidate in pre-clinical and clinical trials.

Several findings have demonstrated that IGF1 participated in regulation of angiogenesis and cell proliferation for the development of DM and neopathy.[33–36] IGF1 inhibition was reported to suppress microvascular endothelial cells growth and invasion in type 2 diabetes.[33] IGF1 and its related factors, for instance lncRNA IGF2AS, were associated with advancement of angiogenesis in type 2 diabetes.[35,36] IGF also was a target of miRNAs in DM-related pathological conditions.[18,37–39] miR-503, miR-18b, miR-29a, or miR-7-modulated cell proliferation/growth or apoptosis via targeting IGF1 expression under HG treatment.[18,37–39] Our present data identified

that IGF1 was a direct target of miR-142-5p in DR and its downstream signaling pathways also participated in modulation of cell proliferation and tissue damages. IGF1/IGF1R-mediated signaling activation was involved in HG-simulated pathological cell and animal models.[18,40] For instance, IGF1/IGF1R were initiated by decreased miR-18b expression that activated downstream phosphorylation of Akt, MEK and ERK, and VEGF transcription in HG-treated HRECs.[18] We found that IGF1/p-IGF1R was activated by the reduced miR-142-5p level in DR. Subsequently, phosphorylation status of IGF/IGF1R downstream proteins, including p-MEK, p-AKT, and p-MEK, were elevated along with VEGF activation, eventually giving rise to cell proliferation. Nevertheless, investigations regarding the cell proliferation markers are still required for further exploration under miR-142-5p restoration or IGF1 knockdown in retinal tissues in the DR-treated rats. Besides IGF1 signaling pathway, other cell proliferation–related signaling pathway should to be verified whether related to miR-142-5p under DR condition.

Conclusion

In conclusion, miR-142-5p was down-regulated and promoted HREC proliferation in response to DR conditions via inhibiting IGF1/p-IGF1R signaling pathway, which pathological effects on retinal tissue in DR rats were relieved by miR-142-5p overexpression or IGF silencing. This miR-142-5p/IGF1 axis facilitate better understanding of the pathogenesis of DR, therefore shedding lights on miR-142-50 as new therapeutic target for DR treatment from bench to clinic.

Animal welfare

This study followed the Guide for the Care and Use of Laboratory Animals for humane animal treatment and complied with relevant legislation.

Authors' contributions

X.M.L. conceived and designed the experiments, J.C.L. analyzed and interpreted the results of the experiments, X.F.L. performed the experiments.

Availability of data and materials

All data generated or analyzed during this study are included in this published article.

Declaration of conflicting interests

The author(s) declared no potential conflicts of interest with respect to the research, authorship, and/or publication of this article.

Ethics approval

Ethical approval for this study was obtained from the Animal Care and Use Committee of the Affiliated Huaian NO.1 People's Hospital of Nanjing Medical University.

Funding

The author(s) received no financial support for the research, authorship, and/or publication of this article.

ORCID iD

Xiuming Liu https://orcid.org/0000-0002-6834-0891

References

1. Kowluru RA, Zhong Q, Santos JM, et al. (2014) Beneficial effects of the nutritional supplements on the development of diabetic retinopathy. *Nutrition & Metabolism* 11(1): 8.
2. Le JT, Hutfless S, Li T, et al. (2017) Setting priorities for diabetic retinopathy clinical research and identifying evidence gaps. *Ophthalmology: Retina* 1(2): 94–102.
3. Zimmet PZ, Magliano DJ, Herman WH, et al. (2014) Diabetes: A 21st century challenge. *The Lancet: Diabetes & Endocrinology* 2(1): 56–64.
4. Wert KJ, Mahajan VB, Zhang L, et al. (2016) Neuroretinal hypoxic signaling in a new preclinical murine model for proliferative diabetic retinopathy. *Signal Transduction and Targeted Therapy* 1: 16005.
5. Couturier A, Dupas B, Guyomard JL, et al. (2014) Surgical outcomes of florid diabetic retinopathy treated with antivascular endothelial growth factor. *Retina (Philadelphia, PA)* 34(10): 1952–1959.
6. Hagiwara S, McClelland A and Kantharidis P (2013) MicroRNA in diabetic nephropathy: Renin angiotensin, aGE/RAGE, and oxidative stress pathway. *Journal of Diabetes Research* 2013: 173783.
7. Wu H, Kong L, Zhou S, et al. (2014) The role of microRNAs in diabetic nephropathy. *Journal of Diabetes Research* 2014: 920134.
8. Schirle NT, Sheu-Gruttadauria J and MacRae IJ (2014) Structural basis for microRNA targeting. *Science (New York, N.Y.)* 346(6209): 608–613.
9. Shrestha A, Mukhametshina RT, Taghizadeh S, et al. (2017) MicroRNA-142 is a multifaceted regulator in organogenesis, homeostasis, and disease. *Developmental Dynamics: An Official Publication of the American Association of Anatomists* 246(4): 285–290.

10. Sladitschek HL and Neveu PA (2015) The bimodally expressed microRNA miR-142 gates exit from pluripotency. *Molecular Systems Biology* 11(12): 850.
11. Mildner A, Chapnik E, Manor O, et al. (2013) Mononuclear phagocyte miRNome analysis identifies miR-142 as critical regulator of murine dendritic cell homeostasis. *Blood* 121(6): 1016–1027.
12. Sharma S (2017) Immunomodulation: A definitive role of microRNA-142. *Developmental and Comparative Immunology* 77: 150–156.
13. Wu JH, Gao Y, Ren AJ, et al. (2012) Altered microRNA expression profiles in retinas with diabetic retinopathy. *Ophthalmic Research* 47(4): 195–201.
14. Shigematsu S, Yamauchi K, Nakajima K, et al. (1999) IGF-1 regulates migration and angiogenesis of human endothelial cells. *Endocrine Journal* 46(Suppl.): S59–S62.
15. Philippou A, Maridaki M, Pneumaticos S, et al. (2014) The complexity of the IGF1 gene splicing, posttranslational modification and bioactivity. *Molecular Medicine (Cambridge, Mass)* 20: 202–214.
16. Jehle PM, Jehle DR, Mohan S, et al. (1998) Serum levels of insulin-like growth factor system components and relationship to bone metabolism in type 1 and type 2 diabetes mellitus patients. *The Journal of Endocrinology* 159(2): 297–306.
17. Brausewetter F, Jehle PM, Jung MF, et al. (2001) Microvascular permeability is increased in both types of diabetes and correlates differentially with serum levels of insulin-like growth factor I (IGF-I) and vascular endothelial growth factor (VEGF). *Hormone and Metabolic Research = Hormon- und Stoffwechselforschung = Hormones et metabolisme* 33(12): 713–720.
18. Wu JH, Wang YH, Wang W, et al. (2016) MiR-18b suppresses high-glucose-induced proliferation in HRECs by targeting IGF-1/IGF1R signaling pathways. *The International Journal of Biochemistry & Cell Biology* 73: 41–52.
19. Hendrick AM, Gibson MV and Kulshreshtha A (2015) Diabetic retinopathy. *Primary Care* 42(3): 451–464.
20. Beltrami C, Angelini TG and Emanueli C (2015) Noncoding RNAs in diabetes vascular complications. *Journal of Molecular and Cellular Cardiology* 89(Pt. A): 42–50.
21. Shafabakhsh R, Aghadavod E, Mobini M, et al. (2018) Association between microRNAs expression and signaling pathways of inflammatory markers in diabetic retinopathy. *Journal of Cellular Physiology* 234: 7781–7787.
22. Satari M, Aghadavod E, Mobini M, et al. (2018) Association between miRNAs expression and signaling pathways of oxidative stress in diabetic retinopathy. *Journal of Cellular Physiology* 234: 8522–8532.
23. Zhang W, Chen S and Liu ML (2018) Pathogenic roles of microvesicles in diabetic retinopathy. *Acta Pharmacologica Sinica* 39(1): 1–11.
24. Qiu F, Tong H, Wang Y, et al. (2018) Inhibition of miR-21-5p suppresses high glucose-induced proliferation and angiogenesis of human retinal microvascular endothelial cells by the regulation of AKT and ERK pathways via maspin. *Bioscience, Biotechnology, and Biochemistry* 82(8): 1366–1376.
25. Wang J, Zhang J, Chen X, et al. (2018) miR-365 promotes diabetic retinopathy through inhibiting Timp3 and increasing oxidative stress. *Experimental Eye Research* 168: 89–99.
26. Zhang X, Yang Y and Feng Z (2018) Suppression of microRNA-495 alleviates high-glucose-induced retinal ganglion cell apoptosis by regulating Notch/PTEN/Akt signaling. *Biomedicine & Pharmacotherapy = Biomedecine & Pharmacotherapie* 106: 923–929.
27. Liu HN, Cao NJ, Li X, et al. (2018) Serum microRNA-211 as a biomarker for diabetic retinopathy via modulating Sirtuin 1. *Biochemical and Biophysical Research Communications* 505(4): 1236–1243.
28. Xia F, Sun JJ, Jiang YQ, et al. (2018) MicroRNA-384-3p inhibits retinal neovascularization through targeting hexokinase 2 in mice with diabetic retinopathy. *Journal of Cellular Physiology* 234(1): 721–730.
29. Yao J, Wang J, Yao Y, et al. (2018) miR-133b regulates proliferation and apoptosis in high-glucose-induced human retinal endothelial cells by targeting ras homolog family member A. *International Journal of Molecular Medicine* 42(2): 839–850.
30. Yang C, Tahiri H, Cai C, et al. (2018) microRNA-181a inhibits ocular neovascularization by interfering with vascular endothelial growth factor expression. *Cardiovascular Therapeutics* 36(3): e12329.
31. Elgheznawy A, Shi L, Hu J, et al. (2015) Dicer cleavage by calpain determines platelet microRNA levels and function in diabetes. *Circulation Research* 117(2): 157–165.
32. Zhang Q, Xiao X, Li M, et al. (2014) miR-375 and miR-30d in the effect of chromium-containing Chinese medicine moderating glucose metabolism. *Journal of Diabetes Research* 2014: 862473.
33. Li Z, Jiang R, Yue Q, et al. (2017) MicroRNA-29 regulates myocardial microvascular endothelial cells proliferation and migration in association with IGF1 in type 2 diabetes. *Biochemical and Biophysical Research Communications* 487(1): 15–21.
34. Yan L, Xie M, Lu H, et al. (2018) Anti-apoptotic effect of IGF1 on Schwann exposed to hyperglycemia is mediated by neuritin, a novel neurotrophic factor. *Molecular Neurobiology* 55(1): 495–505.
35. Ribot J, Caliaperoumal G, Paquet J, et al. (2017) Type 2 diabetes alters mesenchymal stem cell secretome

composition and angiogenic properties. *Journal of Cellular and Molecular Medicine* 21(2): 349–363.
36. Zhao Z, Liu B, Li B, et al. (2017) Inhibition of long noncoding RNA IGF2AS promotes angiogenesis in type 2 diabetes. *Biomedicine & Pharmacotherapy = Biomedecine & Pharmacotherapie* 92: 445–450.
37. Hou LJ, Han JJ and Liu Y (2018) Up-regulation of microRNA-503 by high glucose reduces the migration and proliferation but promotes the apoptosis of human umbilical vein endothelial cells by inhibiting the expression of insulin-like growth factor-1 receptor. *European Review for Medical and Pharmacological Sciences* 22(11): 3515–3523.
38. Han C, Chen X, Zhuang R, et al. (2015) miR-29a promotes myocardial cell apoptosis induced by high glucose through down-regulating IGF-1. *International Journal of Clinical and Experimental Medicine* 8(8): 14352–14362.
39. Wang B, Sun F, Dong N, et al. (2014) MicroRNA-7 directly targets insulin-like growth factor 1 receptor to inhibit cellular growth and glucose metabolism in gliomas. *Diagnostic Pathology* 9: 211.
40. Gong Y, Ma Y, Sinyuk M, et al. (2016) Insulin-mediated signaling promotes proliferation and survival of glioblastoma through Akt activation. *Neuro-Oncology* 18(1): 48–57.